A NEW METHOD BASED ON TEMPLATE REGISTRATION AND DEFORMABLE MODELS FOR PELVIC BONES SEMI-AUTOMATIC SEGMENTATION IN PEDIATRIC MRI

A. Virzì[1,2], *J.-B. Marret*[2], *C. O. Muller*[2], *L. Berteloot*[2], *N. Boddaert*[2], *S. Sarnacki*[2], *I. Bloch*[1]

[1] LTCI, Télécom ParisTech, Université Paris-Saclay, Paris, France.
[2] Departments of Pediatric Surgery and Radiology, Necker-Enfants Malades Hospital, APHP, Paris Descartes University, PRES Sorbonne Paris Cité, INSERM, Institut Imagine, Paris, France.

ABSTRACT

In this paper we address the problem of bone segmentation in MRI images of children, in the region of the pelvis. To cope with the complex structure of the bones in this region and their changing topology during growth, we propose a method relying on 3D bone templates. These models are built from 3D CT images. For a given MRI volume, the closest template is chosen and registered on the MRI data. This leads to an initial segmentation which is then refined using a deformable model approach, where the regularization parameters depend on the local curvature, and the landmarks used during the registration are fixed anchors during the deformation. This approach was successfully applied to 15 MRI volumes of children between 1 and 18 years old, with an average accuracy in terms of medium distance of $MD = 1.17 \pm 0.29\, mm$ and Dice Index of $DC = 0.81 \pm 0.04$.

Index Terms— Pelvic Bones, Pediatric MRI, 3D Segmentation, Template Registration, Deformable Models.

1. INTRODUCTION

Surgical planning relies on the patient's anatomy, and is often based on medical images acquired before the surgery. This is in particular the case for pelvic surgery on children, for various indications such as malformations or tumors. In this particular anatomical region, due to its high vascularization and innervation, a good surgical planning is extremely important to avoid potential functional damages to the patient's organs that could strongly affect their quality of life.
In clinical practice the standard procedure is still to visually analyze, slice by slice, the images of the pelvic region. This task, even if quite easily performed by the expert radiologists, is difficult and tedious for the surgeons due to the complexity and variability of the anatomical structures and hence their images. Moreover, due to specific anatomy depending on the age of the patient, all the difficulties of the surgical planning are emphasized in the case of children, and a clear anatomical understanding is even more important than for the adults. For these reasons it is very important and challenging to provide the surgeons with patient-specific 3D reconstructions, obtained from the segmentation of anatomical images. In particular in the pelvis, MRI is the image modality of choice as a non-irradiating alternative to CT thanks to its better contrast resolution of the soft tissues.

In this paper, we address the problem of segmentation of pelvic bones, which constitutes a core structure that serves as a spatial reference for the surgical planning and 3D visualization of pediatric tumors and malformations.

Concerning the analysis and the segmentation of the pelvic bones structures, computed tomography (CT) is the most widely used imaging modality and many successful methods were developed for adult patients. Most of these studies, due to the complexity of the target structures, introduce strong prior anatomical knowledge represented as atlases [1, 2, 3] or statistical shape models (SSM) [4, 5, 6, 7]. These works are generally difficult to extend to the pediatric population, due to the strong variability in terms of shape and connectivity of the pelvic bones depending on the age of the patient [8]. For this reason, the few studies specifically dedicated to the segmentation of the pelvic bones on pediatric CT images used mostly intensity-based approaches [8]. However, while MRI is preferable for children, these methods do not extend easily to MRI, one of the difficulties being the heterogeneous signal of the bones. Only few studies dealt with the segmentation of the bones on MRI and the ones dealing with the pelvic region were successfully carried out on adult patients, using again shape priors as SSM [9, 10].

In order to overcome the problems of the existing methods, we propose a semi-automatic approach for the segmentation of the pelvic bones in pediatric MRI. In particular, we propose a multi-template based approach, in which the different templates are representative of the different growing phases of the bone structures. The problem of variability in terms of connectivity is then solved by the choice of the closest bone template, and the shape variability is managed by a landmark-based user interaction. A semi-automatic approach was preferred to a fully automatic one, giving to the user a better control on the final segmentation result and avoiding potential unexpected results in case of strong abnormalities of the patient anatomy. To the best of our knowledge, this is the first study specifically addressing the segmentation of pelvic bones in pediatric MRI.

2. PROPOSED SEGMENTATION METHOD

Due to the complexity of the bones in the pelvic regions and their high variability during growth, we propose a multi-template based approach. The idea is to build a set of 3D bone templates at different ages, and to segment images of a patient by using the template corresponding to the closest age. The segmentation is performed in two steps. First, a semi-automatic pre-segmentation is based on the registration of the chosen anatomical bones template to the target MRI. In the second step, the pre-segmentation is refined through the evolution of deformable models, in order to extract the final segmentation.

2.1. Generation of anatomical templates

In order to cope with the high variability in terms of connectivity of the children bones structure during their growth, we propose to build

978-1-5090-1172-8/17/$31.00

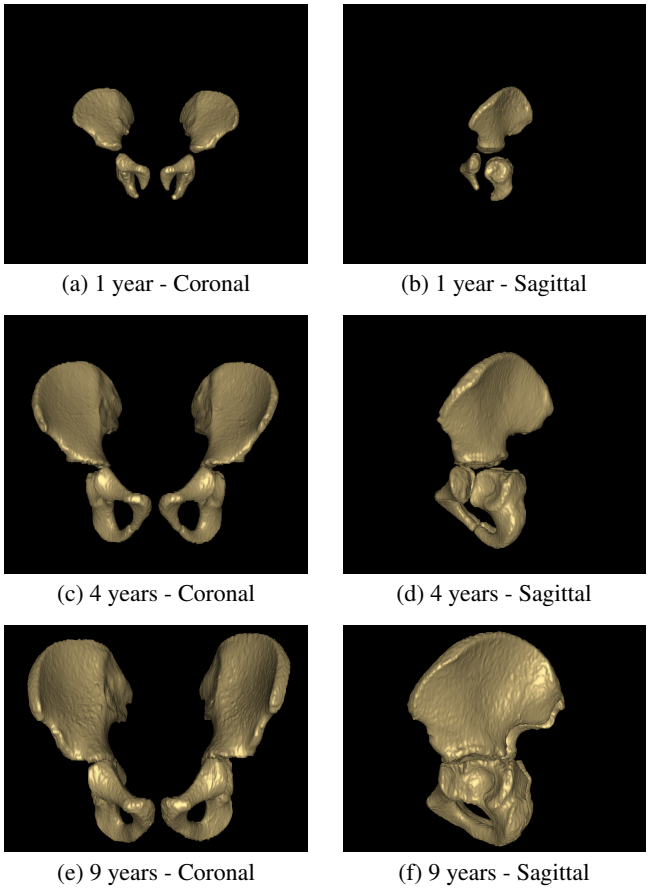

(a) 1 year - Coronal (b) 1 year - Sagittal

(c) 4 years - Coronal (d) 4 years - Sagittal

(e) 9 years - Coronal (f) 9 years - Sagittal

Fig. 1. Examples of 3D bones templates for different ages (coronal and sagittal views).

bones templates from the pelvic CT exams of a few patients of different ages and sex. Although MRI is often the preferred modality for children, CT data are available for enough cases, and allow for an easy, accurate and fast segmentation of the bones. Note that this was done only for a few cases at different ages based on existing data from abdomino-pelvic CT performed for extrapelvian and extraosseous pathologies and no specific CT acquisition was done for this study. To segment the CT volumes, we use the semi-automatic region competition method by Zhu and Yuille [11] implemented in ITK-Snap[1] software [12]. Potential errors on the segmentation results are manually corrected.

Using this method, five anatomical templates (corresponding to 1, 2, 4, 9 and 15 years old children) were generated for each sex group, yielding a total of 10 templates. The different ages of the patients were chosen after analyzing a large dataset of CT scans, to extract the age ranges corresponding to the most significant anatomical changes during the ossification process and growth. Some 3D views of some anatomical templates are shown in Figure 1. The variation in terms of connectivity of the pelvic bones during the growth is given by the gradual fusion of the three structures of the hip bone (ilium, ischium and pubis).

[1]http://www.itksnap.org

2.2. Pre-segmentation from closest template registration

The pre-segmentation of the MRI volumes is obtained through the thin-plate spline (TPS) registration [13] between the chosen anatomical template and the target MRI volume. For each target MRI, in order to have a good representation of the bone connectivity, the template with the corresponding sex and the closest age was chosen.

The TPS-based registration method [13] manages the deformation of an image M, considered as a grid structure, as an interpolation problem. Given two sets of points P_s and P_t in the grid, the optimal non-linear transformation T is obtained by ensuring the point-wise correspondence between the two sets [14]. The propagation of the deformation to the rest of the image grid is defined by the thin-plate interpolation model, that minimizes the bending energy [15].

In our application the image M is the template image, the set P_s represents manually selected landmarks on the template image and the set P_t represents the anatomically corresponding landmarks manually selected on the target MRI I. The pre-segmentation of the bones is then the image $M_t = T(M)$ resulting from the registration.

2.3. Refined segmentation using deformable models

The final segmentation of the bone structures relies on a parametric deformable model, initialized by the pre-segmentation M_t. An original feature of the proposed approach is that the landmarks used for the registration constrain the evolution of the surface. We use the following notations: I is the MRI volume, surfaces are parametrized by (s, r), $v(s, r)$ denotes a point of the evolving surface, and $v_0(s, r)$ the corresponding point on the initial surface given by M_t.

2.3.1. Deformable model

Given a parametric surface $v(s, r) = [x(s, r), y(s, r), z(s, r)]$, the evolution of the deformable model can be formulated starting from a force balance equation $F_{int} + \gamma F_{ext} = 0$, where $F_{int} = \alpha F_{el} + \beta F_{rig}$, F_{el} and F_{rig} are the membrane and the thin-plate forces, respectively [16].

We propose to make the parameters α and β locally dependent on the curvature terms of the initialization of the model $v_0(s, r) = v(s, r) \mid_{t=0}$, and then to keep these values during the model evolution:

$$\alpha(s,r) = \frac{\kappa_\alpha}{\sqrt{\left(\frac{\partial v_0(s,r)}{\partial s}\right)^2 + \left(\frac{\partial v_0(s,r)}{\partial r}\right)^2}} \quad (1)$$

$$\beta(s,r) = \frac{\kappa_\beta}{\sqrt{\left(\frac{\partial^2 v_0(s,r)}{\partial s^2}\right)^2 + 2\left(\frac{\partial^2 v_0(s,r)}{\partial s \partial r}\right)^2 + \left(\frac{\partial^2 v_0(s,r)}{\partial r^2}\right)^2}} \quad (2)$$

where κ_α and κ_β are two constant parameters. These formulations of the parameters α and β allow us to maintain the shape of $v(s, r)$ consistent with the shape of $v_0(s, r)$, during its evolution. Since bones contain both strong and low curvature regions, this characteristic is taken into account in the proposed method, which would not be possible with constant parameters. This approach assumes that, having an initialization close enough to the desired final configuration, the points of the evolving surface $v(s, r)$ will converge to final points that anatomically correspond to the ones of the initialization $v_0(s, r)$. This hypothesis is satisfied thanks to the first template registration step, that provides a good initialization. This allows defining α and β from the curvature on the initial surface v_0.

The external force F_{ext} is chosen classically as the GVF force field [17], but computed from a filtered image volume I_{op}, resulting from a morphological opening of the image I (using a sphere of

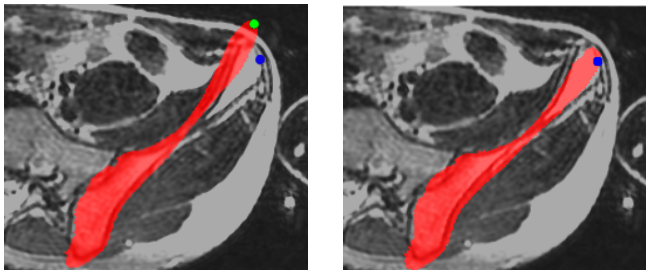

(a) Pre-deformation (b) Post-deformation

Fig. 2. Example of a couple of landmark points and the resulting deformation on a MRI slice portion. The red region represents the current bone template mask. The landmarks are represented by green (P_s) and blue (P_t) points in the images.

radius $r = 2$ mm as structuring element). This allows attenuating the image gradients generated by the small components of adipose tissues close to the target bones regions.

2.3.2. Constraints on the surface evolution

In order to manage the thin-plate registration (see Section 2.2), the most efficient approach for the selection of the landmarks P_s and P_t is to select them on the external borders of the bones structures, as shown in the example in Figure 2, at anatomical positions that are easy to identify. Therefore it is possible to assume that the points P_t, being part of the initialization $v_0(s,r)$, are already at the correct spatial positions for the final segmentation, and thus have to be considered as fixed points during the evolution of $v(s,r)$. Moreover, in order to cope with situations where a point of P_t (manually selected landmarks) could potentially not be exactly in correspondence with a point of the surface $v_0(s,r)$, the fixed points are chosen as the closest points of $v_0(s,r)$ to the points P_t.

3. RESULTS

The proposed method was tested on T2 weighted volumetric MRI, acquired in the coronal plane, of 15 patients between 1 and 18 years old[2]. The full dataset is composed by two subsets of images, respectively made up of 8 and 7 images, with different sizes and resolutions: the first subset ($TE = 59\,ms, TR = 5716\,ms, FA = 90°$) contains images of size $512 \times 512 \times Nz_1$, where Nz_1 varies between 128 and 224, with a voxel size of $0.74 \times 0.74 \times 0.70\,mm^3$; the second subset ($TE = 62\,ms, TR = 2609\,ms, FA = 90°$) contains images with size $256 \times 256 \times Nz_2$, where Nz_2 varies between 204 and 244, with a voxel size of $1.09 \times 1.09 \times 0.70\,mm^3$. The analyzed images did not contain susceptibility artifacts that had a relevant impact on the image quality but, especially on the youngest patients, some motion artifact (even if limited due to the mild sedation of the patients) were present.

In our experiments, the selection of the landmarks was done in an iterative approach in which, for each new landmark selected, the user was able to visualize the deformed template resulting from all the landmarks previously selected. In this way the user, having no prior constraint on the number of landmarks and a clear visualization of the deformation effects, was able to fully control the registration procedure in order to achieve the desired result. This was shown to be very efficient, and the feedback from the users was very positive.

[2]All the images used in this study have been acquired in clinical routine protocols, with approval of the ethics board, and informed consent of patients and patients' parents.

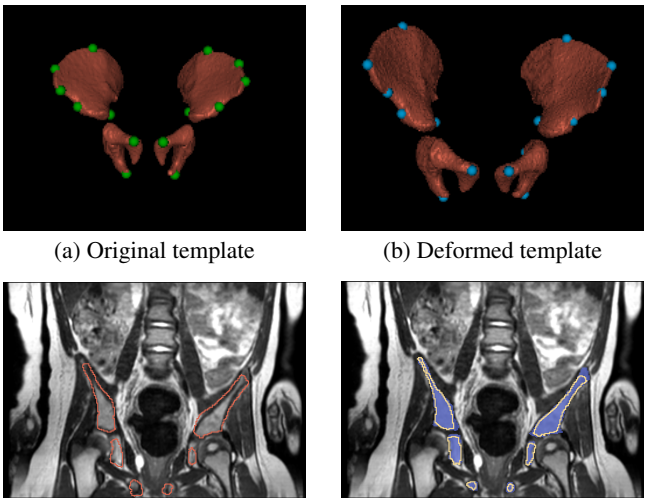

(a) Original template (b) Deformed template

(c) Pre-segmentation (d) Final segmentation

Fig. 3. Example of segmentation results on a 1 year old patient. (a) Original template and source landmarks (green spheres). (b) Deformed template and target landmarks (blue spheres). (c) MRI slice with pre-segmentation (red contour). (d) MRI slice with final segmentation (yellow contour) and manual segmentation (blue mask).

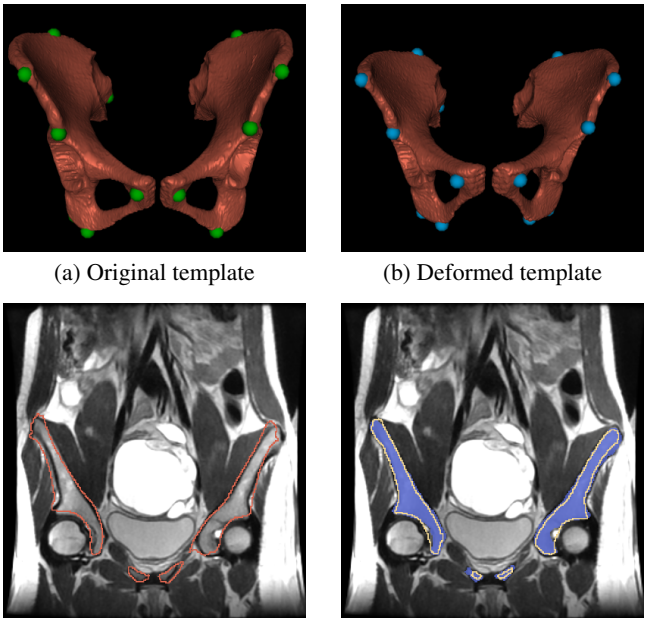

(a) Original template (b) Deformed template

(c) Pre-segmentation (d) Final segmentation

Fig. 4. Example of segmentation results on a 16 years old patient. (a) Original template and source landmarks (green spheres). (b) Deformed template and target landmarks (blue spheres). (c) MRI slice with pre-segmentation (red contour). (d) MRI slice with final segmentation (yellow contour) and manual segmentation (blue mask).

On the tested cases, an average of 20 landmarks (selected as anatomically relevant points) were needed in order to manage the thin-plate registration and to obtain a good initialization for the next step.

The interaction time needed for the registration step was variable in function of the experience of the user: from around 10 min for an expert user to a maximum of 30 min for a new user (less than 5 full registration experiences), and this time decreases rapidly with more experience.

The parameters for the evolution of the deformable model were experimentally set to: $\kappa_\alpha = 0.018$; $\kappa_\beta = 0.01$; $\gamma = 3$. The same parameters were used for the full MRI dataset.

The performances of the proposed approach were validated through comparison with manual segmentations performed by experts, in terms of Dice Index (DC) and Mean Distance (MD) between the proposed segmentation and the manual segmentation. On the whole data base, the following average results were obtained: $DC = 0.81 \pm 0.04$ and $MD = 1.17 \pm 0.29\, mm$. These results are very good, given the resolution of the images, and were positively appreciated by medical experts.

Two examples of the complete segmentation pipeline on a 1 year old patient and on a 16 years old patient are shown in Figure 3 and in Figure 4, respectively. We can see from the results that the proposed method allows us to obtain good segmentation results. Moreover, thanks to the user's control on the landmarks selection, the method is applicable to patients with strong anatomical deformations.

4. CONCLUSION

In this paper, we proposed a semi-automatic method for 3D segmentation of pelvic bones in pediatric MRI volumes. The method relies on two original features. First, a small series of templates is built from CT data, and are used to initialize the segmentation under user's control. Then a second automatic step refines the segmentation using a deformable model in which regularization parameters depend on the local curvature of the bones. This is relevant since pelvic bones contain both almost flat zones and strong curved ones. Qualitative and quantitative results on a varied database of 15 MRI volumes were positively evaluated by medical experts, who appreciated the first manual landmark selection, which was not tedious while guaranteeing a good initialization.

In our future work we plan to change the template selection, and to choose the anatomically closest template instead of the closest age, in order to cope with potential abnormal child development. This method is also planned to be incorporated in a complete segmentation and visualization framework for surgery planning, with an implementation in 3D Slicer software (https://www.slicer.org/).

5. REFERENCES

[1] C. Chu, J. Bai, X. Wu, and G. Zheng, "MASCG: multi-atlas segmentation constrained graph method for accurate segmentation of hip CT images," *Medical Image Analysis*, vol. 26, no. 1, pp. 173–184, 2015.

[2] J. Ehrhardt, H. Handels, W. Plotz, and S.J. Poppl, "Atlas-based recognition of anatomical structures and landmarks and the automatic computation of orthopedic parameters," *Methods of Information in Medicine*, vol. 43, no. 4, pp. 391–397, 2004.

[3] J. Pettersson, H. Knutsson, and M. Borga, "Automatic hip bone segmentation using non-rigid registration," in *IEEE 18th International Conference on Pattern Recognition (ICPR'06)*, 2006, vol. 3, pp. 946–949.

[4] S. Thompson, G. Penney, D. Buie, P. Dasgupta, and D. Hawkes, "Use of a CT statistical deformation model for multi-modal pelvic bone segmentation," in *Medical Imaging*, 2008, vol. SPIE 6914, p. 69141O.

[5] H. Seim, D. Kainmueller, M. Heller, H. Lamecker, S. Zachow, and H. Hege, "Automatic segmentation of the pelvic bones from CT data based on a statistical shape model.," *Eurographics Workshop on Visual Computing for Biomedicine*, pp. 93–100, 2008.

[6] H. Lamecker, M. Seebaß, H. Hege, and P. Deuflhard, "A 3D statistical shape model of the pelvic bone for segmentation," in *Medical Imaging*, 2004, vol. SPIE 5370, pp. 1341–1351.

[7] F. Yokota, T. Okada, M. Takao, N. Sugano, Y. Tada, and Y. Sato, "Automated segmentation of the femur and pelvis from 3D CT data of diseased hip using hierarchical statistical shape model of joint structure," in *International Conference on Medical Image Computing and Computer-Assisted Intervention (MICCAI)*, 2009, vol. LNCS 5762, pp. 811–818.

[8] S. Banik, R. M. Rangayyan, and G. S Boag, "Delineation of the pelvic girdle in computed tomographic images," in *IEEE Canadian Conference on Electrical and Computer Engineering (CCECE 2008)*, 2008, pp. 000179–000182.

[9] J. Schmid and N. Magnenat-Thalmann, "MRI bone segmentation using deformable models and shape priors," in *International Conference on Medical Image Computing and Computer-Assisted Intervention (MICCAI)*, 2008, vol. 5241, pp. 119–126.

[10] J. Schmid, J. Kim, and N. Magnenat-Thalmann, "Robust statistical shape models for MRI bone segmentation in presence of small field of view," *Medical Image Analysis*, vol. 15, no. 1, pp. 155–168, 2011.

[11] S. C. Zhu and A. Yuille, "Region competition: Unifying snakes, region growing, and Bayes/MDL for multiband image segmentation," *IEEE Transactions on Pattern Analysis and Machine Intelligence*, vol. 18, no. 9, pp. 884–900, 1996.

[12] P. Yushkevich, J. Piven, H. Cody, S. Ho, J. C. Gee, and G. Gerig, "User-guided level set segmentation of anatomical structures with ITK-snap," in *NA-MIC/MICCAI Workshop on Open-Source Software*, 2005.

[13] F. L. Bookstein, "Principal warps: Thin-plate splines and the decomposition of deformations," *IEEE Transactions on Pattern Analysis and Machine Intelligence*, vol. 11, no. 6, pp. 567–585, 1989.

[14] F.P.M. Oliveira and J. M. RS Tavares, "Medical image registration: a review," *Computer Methods in Biomechanics and Biomedical Engineering*, vol. 17, no. 2, pp. 73–93, 2014.

[15] M. Holden, "A review of geometric transformations for nonrigid body registration," *IEEE Transactions on Medical Imaging*, vol. 27, no. 1, pp. 111–128, 2008.

[16] C. Xu, A. Yezzi, and J. L. Prince, "A summary of geometric level-set analogues for a general class of parametric active contour and surface models," in *IEEE Workshop on Variational and Level Set Methods in Computer Vision*, 2001, pp. 104–111.

[17] C. Xu and J. L. Prince, "Generalized gradient vector flow external forces for active contours," *Signal Processing*, vol. 71, no. 2, pp. 131–139, 1998.